

RESEARCH ARTICLE

Experimental study on various properties of sustainable, highperformance, and innovative composite (SIFGEO)

Haluk Görkem Alcan¹, Barış Bayrak¹, Ali Öz², Oğuzhan Çelebi², Gökhan Kaplan², Abdulkadir Cüneyt Aydın²

- ¹ Kafkas University, Department of Civil Engineering, Kars, Türkiye
- ² Atatürk University, Department of Civil Engineering, Erzurum, Türkiye

Article History

Received 18 June 2025 Accepted 26 August 2025

Keywords

Alkali-activated concrete Effect of binder High temperature Innovative composite SIFCON Steel fiber

Abstract

This paper focuses on sustainability and innovative materials in the construction industry. The study addresses the mechanical and high-temperature resistance (200 °C, 400 °C, and 600 °C) of SIFGEO, a superior composite material, by combining geopolymer concrete (GPC) and slurry-infiltrated fiber concrete (SIFCON) technologies. Within the scope of the study, the main binder in the SIFGEO specimens is blast furnace slag (BFS), and one group was produced only based on BFS. In the other groups, 10% were added by mass silica fume (SF), metakaolin (MK), and rice husk ash (RHA) instead of slag. As a result of the mechanical tests of the specimens that were not exposed to high temperatures, it was determined that the mixture containing only BFS as a binder had the highest compressive strength, flexural strength, and specific fracture energy. The compressive and flexural strengths of the mixture containing only BFS as a binder were 62.24 and 22.03 MPa, respectively, and the fracture energy was approximately 2146 N/m. The lowest results were obtained in the mixture where RHA was used as a partial replacement for BFS, with compressive strength, flexural strength, and fracture energy measured as 41.31 MPa, 16.81 MPa, and 1346.4 N/m, respectively. The compressive strength, flexural strength, and fracture energy of all mixtures showed a decreasing trend with increasing temperatures. It was observed that dense steel fibers provided effective crack control and increased ductility in both non-high temperature and high temperature exposed samples. In addition, depending on the parameters within the scope of the presented study, the correlation between the experimental results on SIFGEO samples was examined. In addition, statistical analyses were conducted to evaluate the relationships between the mechanical parameters. A strong correlation was found between flexural strength and fracture energy (R2 values between 0.86 and 0.98) and between flexural strength and compressive strength (R2 values between 0.89 and 0.96) for different binder types and temperature conditions. These results confirm that changes in flexural strength are closely linked to both fracture energy and compressive strength in SIFGEO specimens.

^{*} Corresponding author (<u>bbayrak@kafkas.edu.tr</u>)

1. Introduction

Today, the construction industry is constantly searching for new and innovative materials to realize increasingly complex projects [1, 2]. In particular, efforts to increase the flexural strength and ductility of concrete, a brittle material, have been intensifying. This research results in a building material with superior mechanical properties known as SIFCON (slurry-infiltrated fiber concrete). SIFCON combines cement, fine sand, water, and various fibers [3, 4]. The main differences between SIFCON and fibrous concrete (FRC) are the fiber content and production technology. The fiber ratio in fibrous concretes is usually limited to 2%. Studies have determined that more fiber than this ratio damages the strength and workability properties of FRC [5, 6]. Also, FRC may be insufficient in structures or structural elements requiring high strength and durability. SIFCON, which can have a fiber ratio from 3% to 20%, can offer a reasonable solution in such cases [7]. In FRC, the fibers are added to the concrete when fresh, and the mixing is done together. In SIFCON, the fibers are placed in the formwork directionally or randomly. A fluid mortar of cement, fine sand, and water is then infiltrated (poured) over the fibers. Thanks to this manufacturing technology, SIFCON can achieve high fiber ratios. SIFCON is a fibrous composite material. Therefore, the strength of SIFCON depends on the type, ratio, and geometry of the fiber used, as well as the properties of the mortar phase. In addition, the bond (adherence) between the fiber and mortar is another factor that significantly affects the strength of this composite; just like FRC, the fibers in SIFCON act as a bridging under load. Under high stresses, the fibers support the mortar phase and restrict crack formation. SIFCON's high fiber content provides superior tensile strength, impact resistance, toughness, and ductility compared to conventional concrete and FRC [8-10]. SIFCON has various applications in various construction projects thanks to its superior properties. Using SIFCON in structures built to store explosive materials, industrial floors where ductility is a top priority, and floors subjected to intense impact loads, restoration, and reinforcement will be advantageous. In addition, it is possible to produce thinner sections of components exposed to high loads in bridge piers and high-rise structures with SIFCON [11, 12]. Despite the superior properties of SIFCON, there are various disadvantages. The first disadvantage is the loss of strength of cement-based mortar at high temperatures. According to the research, at temperatures above 400°C, spills and extra cracks begin to form in the concrete. After 600°C, a large amount of strength loss occurs as the C-S-H bonds forming the concrete's carrier skeleton weaken and break [13-15]. Another disadvantage of SIFCON is that a high cement dosage is generally used in the mortar phase. In the cement production process, approximately 1 kg of CO₂ gas is emitted into the atmosphere to obtain 1 kg of cement. According to data from the Global Cement and Concrete Association, annual cement production in the world in 2020 was 4.2 billion tons [16]. Based on these data, it is clear that the amount of harmful CO₂ emitted to the atmosphere in cement production is enormous.

The use of sustainable, green, and environmentally friendly materials is essential in today's world. The use of such materials has gained significant momentum in the construction industry, which has a great place in society economically and socially. In this context, geopolymer concrete (GPC) technology has been developed as a result of the search for environmentally friendly and energy-efficient materials as an alternative to traditional building materials [17-19]. Geopolymers are polymeric-based building materials formed by reacting inorganic components with alkaline liquids. Another name for geopolymers is alkaliactivated concrete. Instead of cement, aluminosilicate-based inorganic materials such as fly ash, blast furnace slag, silica fume, metakaolin, rice husk ash, and volcanic glasses are generally used as binders (precursors) in GPC production [20-23]. The majority of these binders are obtained through the recycling of industrial waste. GPC reduces CO2 emissions significantly compared to cementitious building materials due to the waste recycling process. Sodium hydroxide (NaOH), sodium silicate (Na₂SiO₃), and potassium hydroxide (KOH) are mostly used for the activation of inorganic binders in GPC production [24]. Three-dimensional Si-O-Al polymer chains are formed as a result of the reaction of aluminosilicate oxides in inorganic

components and polysilicates in alkaline activators. These chemical reactions between the components are called polymerization. The degree of polymerization of GPC depends on the binder and activator content, binder/activator ratio, and curing conditions [25, 26]. GPC is becoming increasingly popular due to its sustainability, as it is produced from industrial waste recycling and requires significantly less energy and carbon emissions than cement production. However, there are other reasons for the great interest in geopolymer concretes. With proper optimization of GPC components, it exhibits superior mechanical and durability properties compared to conventional concrete. Thanks to the three-dimensional bonds formed from the polymerization reaction, GPC has several advantages: resistance to high temperatures, aggressive environments such as acid and base attacks, low conductivity, minimum shrinkage, and early compressive and flexural strength [27-29]. In addition, geopolymer concretes are resistant to chemical and physical corrosion; these properties ensure the long life of the structures. The mechanical and durability properties of a building material are important factors that determine its performance. These properties play a critical role in determining the uses and advantages of the material. GPC has the potential to offer a wide range of applications thanks to its properties. The high mechanical properties of geopolymer concrete and their resistance to high temperatures and chemical corrosion enable them to be used in various areas ranging from industrial plants to infrastructure projects and nuclear waste storage facilities [30-32]. In addition, the fire resistance and insulation properties of geopolymer make it preferred to meet fire safety standards. Due to the advantages above, GPC's usage areas, role, and impact on the construction industry will likely increase with great momentum.

This study combined SIFCON and geopolymer technology to produce a composite material with superior properties. This innovative material (SIFGEO) represents a further step forward in the construction industry. Combining the high strength of SIFCON and the environmentally friendly properties of geopolymer will increase the durability of structures while reducing their environmental impact. In addition, the combined use of these materials will increase the lifespan of traditional structures, primarily by increasing their high-temperature resistance, while also providing economic benefits by reducing maintenance costs. SIFGEO could form the basis for the next generation of green buildings. Combining these materials could set a new standard for sustainability and innovation in the construction industry. As a result, SIFGEO can play an important role in future building projects and lead the construction industry in a more sustainable direction.

In this study, blast furnace slag was the main binder used to produce SIFGEO specimens. To observe the binder effect in the mixtures, silica fume, metakaolin, and rice husk ash were used at 10% by mass instead of slag. To observe the effects of high temperature on SIFGEO specimens, the mixtures were exposed to 200, 400, and 600 °C for 2 hours. After the temperature treatment, the specimens' compressive, flexural, fracture energy, and strength loss properties were measured. In addition, regression analyses were performed on the binder and high-temperature results to investigate the relationship between them. The significance of this research lies in its innovative integration of SIFCON and geopolymer technologies to develop SIFGEO, a sustainable composite material with superior mechanical and thermal performance. This combination not only addresses the urgent need for environmentally friendly construction materials by reducing CO2 emissions through the use of industrial by-products, but also enhances structural performance through high fiber content and improved ductility. In this study, four binder types were examined, and results showed that the mixture containing only blast furnace slag achieved the highest compressive strength (62.24 MPa), flexural strength (22.03 MPa), and fracture energy (2146 N/m) under ambient conditions. Although all mixtures experienced strength losses with increasing temperature, notable residual performance and ductile behavior were maintained even at 600 °C, demonstrating SIFGEO's potential for high-performance and sustainable applications in demanding structural environments.

2. Materials and methods

2.1. Materials

In this study, blast furnace slag (BFS), silica fume (SF), metakaolin (MK), and rice husk ash (RHA) were used as aluminosilicate-based inorganic binders. The average particle sizes of the binders were 30, 0.15, 2, and 10 μ m, respectively. In addition, the specific weights of the inorganic precursors were 2.88, 2.25, 2.65, and 2.28 g/cm³, respectively. The chemical properties of the binders used in the experiments are presented in Table 1.

Fig. 1 presents the X-ray diffraction (XRD) patterns of blast furnace slag (BFS), silica fume (SF), metakaolin (MK), and rice husk ash (RHA) used as binders in the SIFGEO mixtures. BFS shows a predominantly amorphous structure with a broad hump between 25°–35° 2θ, accompanied by crystalline peaks of merwinite, gehlenite, and quartz, indicating its high latent hydraulic reactivity. SF exhibits an almost entirely amorphous pattern with a distinct broad hump between 20°–30° 2θ, consistent with its high SiO₂ content and ultrafine particle size, which can contribute to dense matrix formation but provides limited calcium for C-A-S-H gel formation. MK displays characteristic crystalline peaks of kaolinite derivatives and quartz, along with an amorphous hump between 20°–28° 2θ, reflecting its high Al₂O₃ content and suitability for geopolymerization. RHA shows intense crystalline peaks of quartz due to its high silica content, but the presence of some amorphous regions indicates potential pozzolanic reactivity depending on burning conditions. The differences in crystalline and amorphous phase contents among the binders are expected to significantly influence the polymerization process, gel type formation, and ultimately the mechanical performance of the SIFGEO specimens.

The experiments used sodium silicate (Na₂SiO₃) and sodium hydroxide (NaOH) solutions to activate binders. Both solutions are liquid; Na₂SiO₃ has a specific gravity of 1.4 g/cm³, and NaOH has a specific gravity of 1.22 g/cm³. Approximately 64% of both activators consists of water. The ratio of sodium silicate to sodium hydroxide in the activator solutions was chosen as 2.5, and the solutions were ready 24 hours before the experiments. No plasticizer was added to the groups during the experiments. It was emphasized that the fine aggregate size should be smaller than 600 µm for the mortar phase of SIFCON to envelop the dense fiber volume and spread homogeneously. Therefore, marble powder (MP) with a particle size of less than 200 µm was used in the present study. The specific gravity of MP is 2.66 g/cm³, and its particles are crystalline. The fibers used during the experiments were hooked steel with a length and diameter of 30 mm and 0.5 mm, respectively. The physical and mechanical properties of the fibers are given in Table 2.

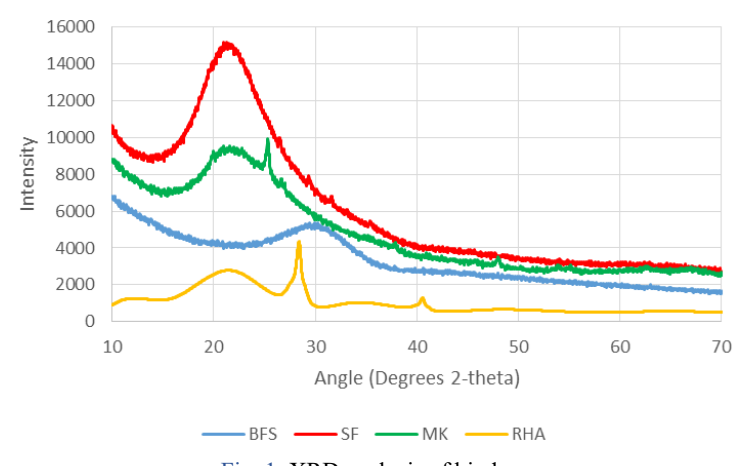


Fig. 1. XRD analysis of binders

Table 1, Physical	and chemical	properties of	hinders (%)
Table I. Physical	and chemical	properties of	Difficiers (70)

Oxides	BFS	SF	MK	RHA
CaO	40.6	0.3	0.8	0.5
SiO_2	35.5	95.8	52.9	86.2
Al_2O_3	11.2	0.3	43.6	0.6
Fe_2O_3	0.7	0.7	0.6	0.4
MgO	10.1	0.8	0.3	0.4
Na ₂ O	0.2	0.3	0.6	0.4
SO_3	0.5	0.2	0.1	0.3
K ₂ O	0.4	0.5	0.1	1.9
LOI	0.6	0.5	0.3	8.9
Unit weight (kg/cm ³)	2880	2250	2650	2250
Color	Cream	Light grey	Off white	Dark grey
Specific surface area (m ² /kg)	415	19500	16500	2125

Table 2. Properties of steel fiber

Туре	Hooked-end
Cross-Section	Circular
Unit weight (kg/m³)	7850
Diameter (mm)	0.5
Length (mm)	30
Aspect ratio (1/d)	60
Tensile strength (MPa)	1100
Elastic modulus (MPa)	205000

2.2. Production of samples and curing

In this study, four groups were created, and the groups vary according to the type of binders. The activator/binder ratio was 0.88 in all groups. The amounts of the mixtures used in the experiments in kg according to 1 m^3 are presented in Table 3.

The fiber volume of SIFGEO specimens was determined to be 8%, and the specimens were produced in two stages. First, half of the fiber to be used in the molds was randomly placed in the mold. For the mortar to surround the fibers and prevent the formation of voids, the mold was vibrated on the shaking table and poured up to half the height of the mold. Then, the remaining fibers were placed in the mold similarly, and mortar was added until the mold was filled. After the casting, the specimens were kept on the shaking table for another 2 minutes to ensure void-free production.

While preparing the SIFGEO mortar, the dry components (binder and marble powder) were first placed in the mixer and mixed for three minutes. After the dry ingredients were homogenously mixed, sodium hydroxide was added to the mixer and mixed for another three minutes. Finally, sodium silicate was added to the mixer, and the mortar was mixed for four more minutes.

Table 3. Mixtures of SIFGEO mortar (kg/m³)						
Component	K1	K2	K3	K4		
BFS	800	720	720	720		
SF	-	80	-	-		
MK	-	-	80	-		
RHA	-	-	-	80		
NaOH	200	200	200	200		
Na ₂ SiO ₃	500	500	500	500		
Marble powder	541	520	535	520		

When fresh mortar was obtained, the flow diameter values of each group were measured as specified in ASTM C230 [33]. The flow diameters of K1, K2, K3, and K4 mixtures were measured as 250, 250, 240, and 220 mm, respectively. In the literature, it has been emphasized in many studies that the strength values increase when heat curing is applied to geopolymer mixtures [34-36]. The heat-curing process was initiated after the production of the test specimens was completed. In this study, the specimens produced for all groups were heat cured at 80 °C for 8 hours to have sufficient mechanical properties [37, 38]. After heat curing, the SIFGEO specimens were removed from the oven and allowed to cool at room temperature. Then, the specimens were removed from the molds, cured at room temperature for 7 days, and the test procedure was started.

2.3. Experimental test procedures

To determine the compressive strength of the produced SIFGEO specimens, a compressive test was performed according to ASTM C349 [39]. The specimens produced for compressive strength are cubes, and the size of one surface is 50 mm. In addition, a three-point flexural test was performed according to ASTM C348 [40] for the flexural strength of the specimens. Plate SIFGEO specimens were produced for flexural strength, and the dimensions of the specimens were 20x60x300 mm. Cube and plate samples produced for the experiments are presented in Fig. 2. Load-deflection graphs of the specimens were created using the data obtained during the flexural test. The fracture energies of the specimens were calculated according to ASTM C1018 [41]. Another test applied within the scope of this study is the high-temperature effect according to ASTM E119 [42]. The cured SIFGEO specimens were placed in an oven that could increase by 10 °C per minute, and then the oven was kept at 200 °C, 400 °C, and 600 °C for 2 hours. Upon completion of the test, the specimens were removed from the oven and allowed to cool at room temperature for 24 hours. The curing and high-temperature process for the samples are presented in Fig. 3. After cooling, the SIFGEO specimens were subjected to the abovementioned compressive and flexural tests.





Fig. 2. Samples produced for testing, and plate and cube samples details

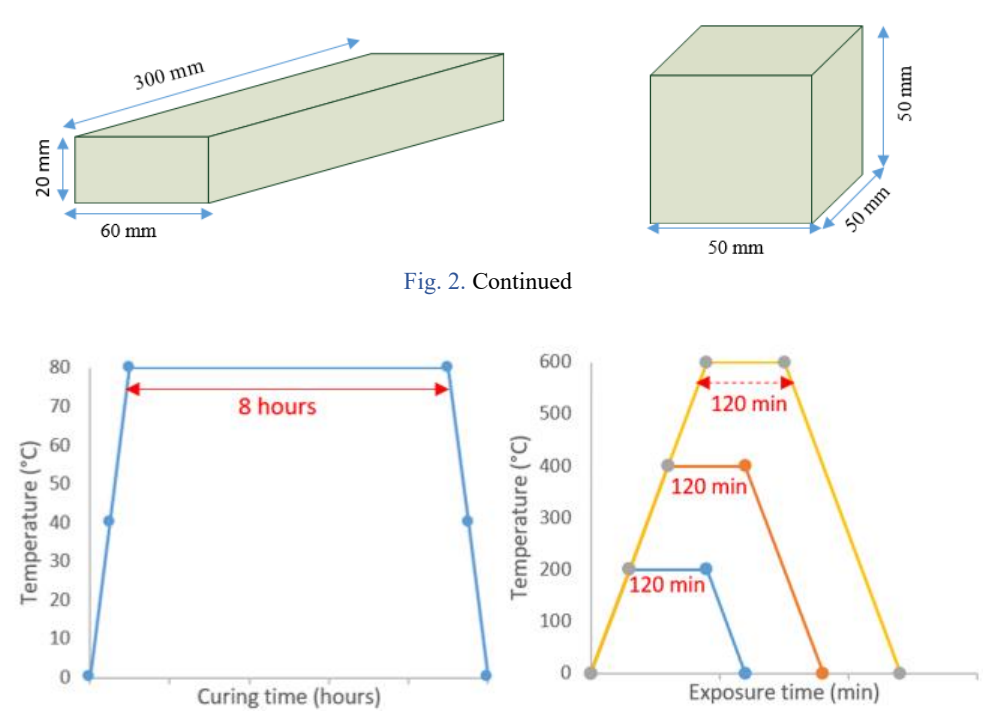


Fig. 3. Heat curing (left) and high temperature (right) processes

3. Result and discussion

3.1. Mechanical effect

Fig. 4 presents the compressive and flexural strengths of SIFGEO specimens without high-temperature application. When the compressive and flexural strengths of the mixtures are analyzed in Fig. 4, it is seen that the highest values belong to the K1 mixture, and the lowest values belong to the K3 mixture. Although the compressive and flexural strengths of K2 and K4 specimens were quite close, they remained at lower levels than the other two groups. The differences in the strength of the groups with the same parameters, such as curing conditions and fiber ratio, were due to the differences in the precursor materials. For example, in the K1 group, where the highest results were observed, only blast furnace slag was used as a binder, and the compressive and flexural strengths were measured as 62.24 and 22.03 MPa, respectively. In group K4, where these values were the lowest, rice husk ash was used with blast furnace slag as a binder. This group's compressive strength was 41.31 MPa, and its flexural strength was 16.83 MPa. The strength differences between the groups can be attributed to the presence of CaO in the BFS and the Si/Al ratio of the binders. When alkalis activate inorganic components, the bearing properties are realized by the presence of NASH gels [43, 44]. In addition to these gels, after the activation of slag, CASH gels are also formed thanks to the CaO structures in their content. The structure of this gel is similar to CSH formed due to the hydration of cement, and this structure makes an extra contribution to its strength [45, 46]. For these reasons, the higher content of BFS as a binder contributed positively to the compressive and flexural strengths. In addition, these results can indicate that the hydration modulus of BFS is higher than that of other binders. Nath and Sarker [47] reported that the mechanical properties of the test specimens increased with increasing the amount of BFS used as a binder in geopolymer mixtures. They stated that the calcium component in BFS forms calcium alumino-silicate hydrate (C-A-S-H) gel due to polymerization. This gel structure contributes to early and high strength. Similarly, Bhavsar and Panchal [48] reported faster hardening and higher compressive strength of geopolymer mixtures due to the CaO in BFS. In addition to the type of binder, another factor affecting the strength can be interpreted as the chemical composition of the binder, i.e., the Si/Al ratio. These results are based on K2, K3, and K4 specimens. Instead of slag, SF, MK, and RHA were added to the K2, K3, and K4 mixtures. These precursors have a low level of CaO in their composition, and their ratios are very close. When the results of these three groups were analyzed, the compressive strength of the K3 mixture was 57.09 MPa, and the flexural strength was 21.21 MPa. The compressive values of the K2 and K4 groups are about 27% lower than K3, and the flexural values are about 20% lower. Due to MK's low Si/Al ratio, Si and Al particles are more evenly distributed. In this way, the strength values are higher due to the formation of more chain-structured Si-O-Al bonds in this mixture. When the chemical contents of SF and RHA used in the K2 and K4 groups are analyzed in Table 1, Si components are considerably higher than Al components. With the high Si/Al ratio of the binders used in these groups, the strengths remain at lower values due to the low amount of bond in the activation process. Wang et al. [49] stated that the mechanical properties of geopolymers decrease as the Si/Al ratio in the precursor content increases. Their study determined that the optimum Si/Al ratio was 1.5 and that mechanical properties decreased when this ratio was exceeded. In their study on Si/Al metakaolin-based geopolymer, He et al. [50] reported that the chemical stability of GPC samples weakened as the Si/Al ratio exceeded 3.

Another remarkable result in Fig. 4 is the high flexural strength of SIFGEO specimens. Plain concrete is a brittle construction material. If previous studies and various standards are evaluated, the flexural strength of plain concrete is approximately 1/10 of the compressive strength, although it varies according to various parameters. GPC is also a brittle material, and the relationship between compressive strength and flexural strength is similar to plain concrete [51-53]. In both fiber-reinforced concrete and fiber-reinforced geopolymer concrete, the flexural-to-compressive strength ratio can be brought to around 1/5 [54-57]. When the ratio of flexural strength to compressive strength of SIFGEO specimens is analyzed, it is seen that it is approximately 1/3 in each group. These superior flexural strength values of the groups are due to the dense fiber volume. In both compressive and flexural tests, the presence of fibers was decisive in the behavior of the specimens. However, the presence of a fiber volume of 8% had the most dominant effect on the flexural strength. For example, the flexural strength of 22 MPa measured in the K1 mix was close to the compressive strength of normal-strength concretes, which is an indication of the superiority of SIFGEO.

Fig. 5(a) shows the load-deflection graphs of SIFGEO specimens after flexural tests. Under flexural loads, the fibers act as a bridge in the mortar phase. The load to which the specimen section is subjected is not only borne by the mortar but also by the fibers. In other words, the energy required for the load to fail the specimen will not only break the mortar phase but also separate the fibers from the mortar microstructure. Thanks to the bridging property provided by the dense fiber volume, the crack formation of SIFGEO specimens under flexural loading was significantly limited, and the development of cracks was restricted. The most apparent indication that the fibers prevented crack formation and propagation in the specimens is after the peak load in the load-deflection graph. Despite the increasing deformation after the maximum load in all groups, the rate of decrease of the load is slow. This can be considered as evidence that SIFGEO specimens exhibit ductile behavior. It is noteworthy in Fig. 5(a) that all groups have approximately the same deflection (33 mm) due to the flexural test. In other words, regardless of the difference in the precursor materials in the mixtures, the dense steel fiber volume similarly improved the behavior of SIFGEO specimens after peak load. In Fig. 5(a), the part that differs between the groups is the curves formed by the load values. These curve values were higher in K1 and K3 specimens and lower in K2 and K4. It was mentioned that the reasons for the difference between the compressive and flexural strengths of the mixtures were due to the type of binder and the chemical composition of the binder. These differences in the load-deflection graph of SIFGEO specimens reflect the same reasons.

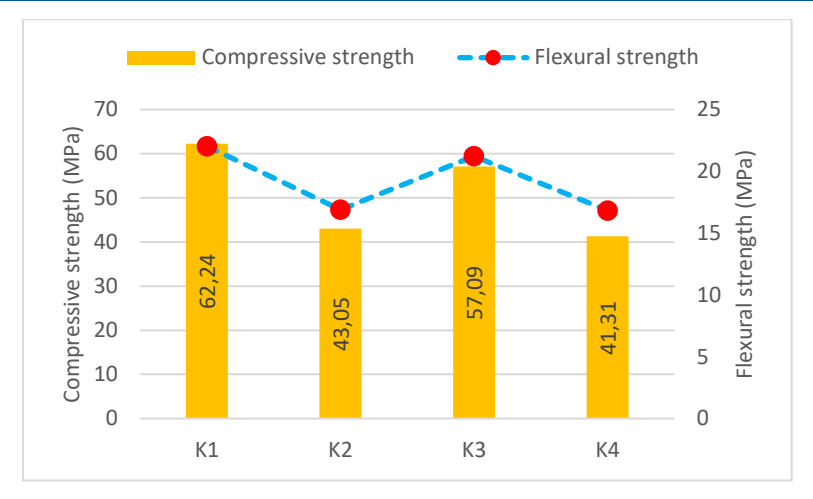


Fig. 4. Compressive and flexural strengths of SIFGEO

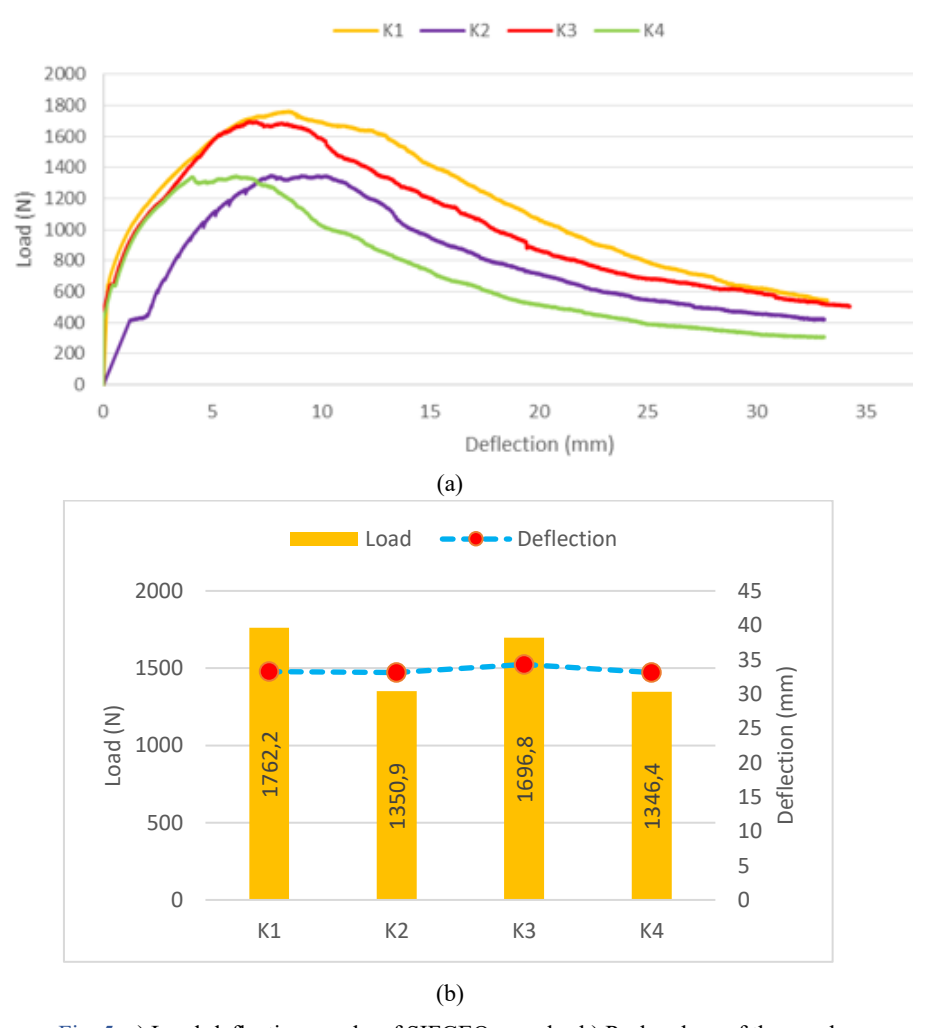
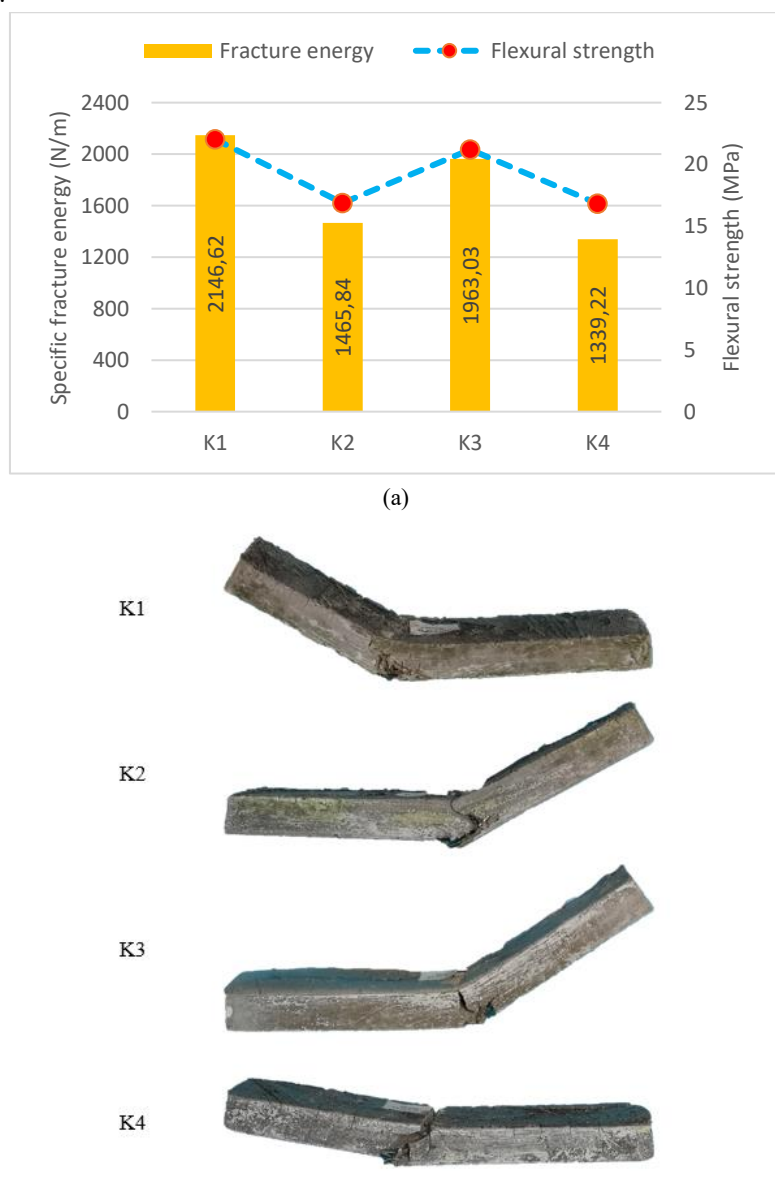


Fig. 5. a) Load-deflection graphs of SIFGEO samples b) Peak values of the graph

In Fig. 5(b), the maximum load and deflection values read from the load-deflection graphs are presented in detail. Gok and Sengul [58] investigated the mechanical properties of geopolymer SIFCON specimens produced from waste steel fibers up to 5% volume. As a result of their experiments, they emphasized that the compressive and flexural strengths increased significantly as the fiber volume increased. İpek et al. [59] conducted experiments on steel fiber SIFCON specimens ranging from 3% to 10% volume using cement as a binder. In their study, they applied different pressure curing values to the specimens. They stated that they reached more than 60 MPa flexural strength with increasing curing pressure. Alcan and Bingöl [60] investigated the mechanical properties of cementitious SIFCON specimens with a fiber volume of 10%, different fiber types, and different matrix phases. As a result of their study, they found that the mechanical properties and behavior of the specimens under load depended on the type of fiber used and the content of the mortar phase.



(b)
Fig. 6. a) Fracture energy and flexural strength of SIFGEO specimens, b) Failure modes of SIFGEO specimens

Fig. 6(a) presents the fracture energy and flexural strength of SIFGEO specimens in the same table. Fracture energy is the total energy a material can absorb before fracture. In this study, the fracture energy of the specimens was measured by three-point bending tests. The fracture energies of each group of SIFGEO specimens were calculated by calculating the total area under the load-deflection graphs given in Fig. 5(a). When the results are analyzed, the highest fracture energy is 2146 N/m, and the lowest value is 1339 N/m for the K1 and K4 groups, respectively. In other words, the fracture energy of the K1 sample is 1.6 times that of K4. The dense fibers in the SIFGEO specimens changed the direction of the crack formed in the section during the bending test and made the crack progression difficult. Crack propagation and the difficulty of new crack formation mean that the energy required to fail the composite increases. The fracture energies of SIFGEO specimens are high due to the fibers' ability to bridge. The load-deflection graphs show that the maximum deflection values of all four groups are approximately the same. In this case, it can be interpreted that the differences between the fracture energies are due to the type of binder or the content of the binder. Considering that the fracture energy is calculated from the load-deflection graph in the flexural test, the relationship between the effect of the binder on the flexural strength and the fracture energy can be understood. The graph shows that the mixtures' flexural strength values and fracture energies are parallel. Another observation in Fig. 6(a) is that SIFGEO specimens exhibit ductile behavior. After the peak load value, the force loss in the specimens occurred slowly, and the end of the experiment was at maximum deformation, not maximum load.

The failure modes of the specimens presented in Fig. 6(b) can be considered as evidence of ductility. In all groups, failure occurred in the form of shear failure at the maximum moment value, i.e., approximately at the midpoint of the specimens. Due to the dense fiber structure, the specimens were not brittle fractured and could not carry the load in one piece, even after a significant deflection. Many researchers have studied the fracture energy of steel fiber-reinforced concrete and geopolymers. In these studies, significant increases in fracture energy were observed with the addition of fibers in both composites. It was stated that the fracture energy increased due to the increase in flexural strength, due to the adherence of the fibers to the mortar/concrete. In addition, it was observed that the deflection values of the test specimens increased significantly and exhibited more ductile behavior due to the bridging properties of the fibers [61-66].

3.2. High temperature effect

Fig. 7 shows the compressive and flexural strengths of SIFGEO mixtures exposed to high temperatures of 200, 400, and 600 °C, respectively. In addition, Fig. 8 shows the strength losses at these temperatures. As can be seen from the graphs, the highest compressive strengths after three high-temperature treatments were measured in the K1 mix, where only furnace slag was used as a binder. Based on these data, it can be interpreted that the high-temperature resistance of BFS is better than that of the other precursors. The above section mentioned that more polymeric bonds were formed in the mixtures where only slag was used due to the CaO in the microstructure. It can be interpreted that the high number of these bonds forming the carrier skeleton of SIFGEO reduced the degradation of the composite after high temperatures. The flexural strength results were generally similar to the compressive strength, but the flexural strength of the K3 mixture at 400 °C (10.8 MPa) was slightly outside this similarity. This was thought to be because the degradation of metakaolin in the K3 mixture was less at this temperature than in the other precursors. This difference disappeared at 600 °C.

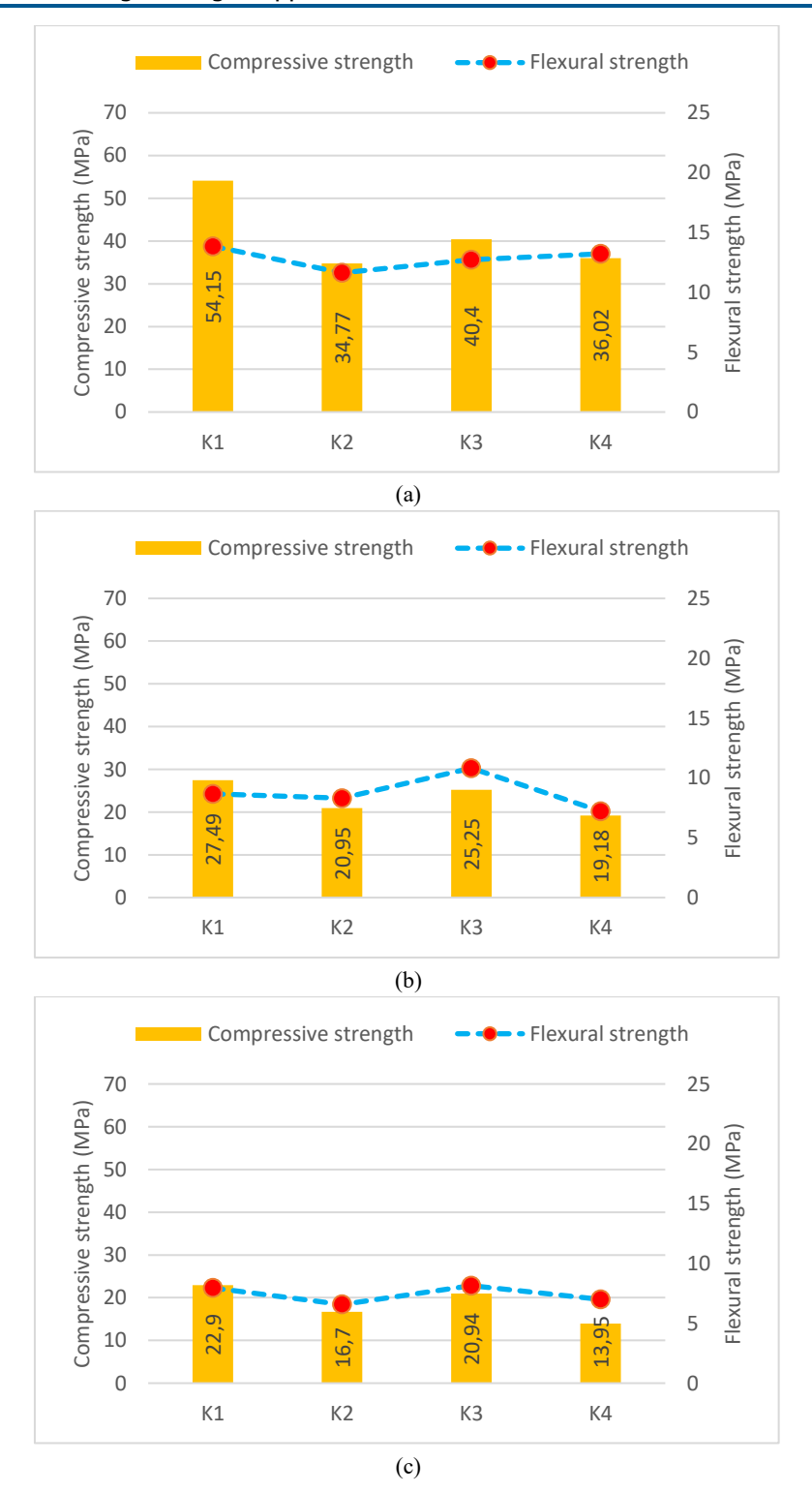
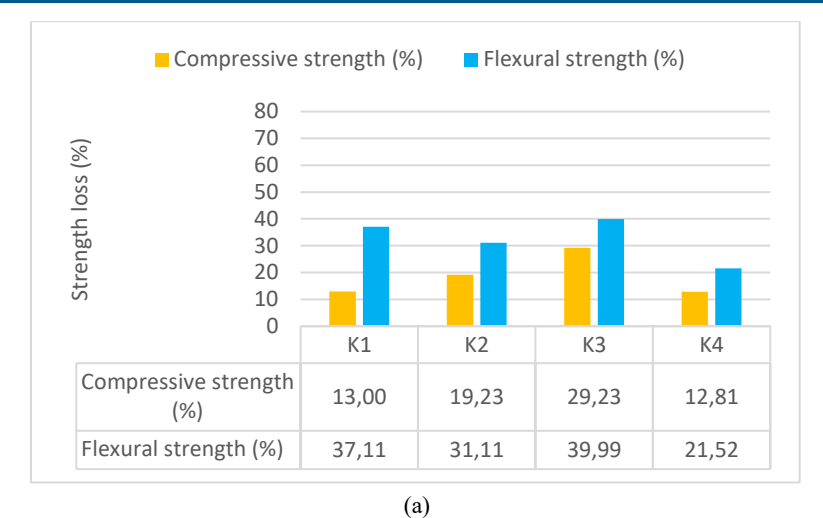
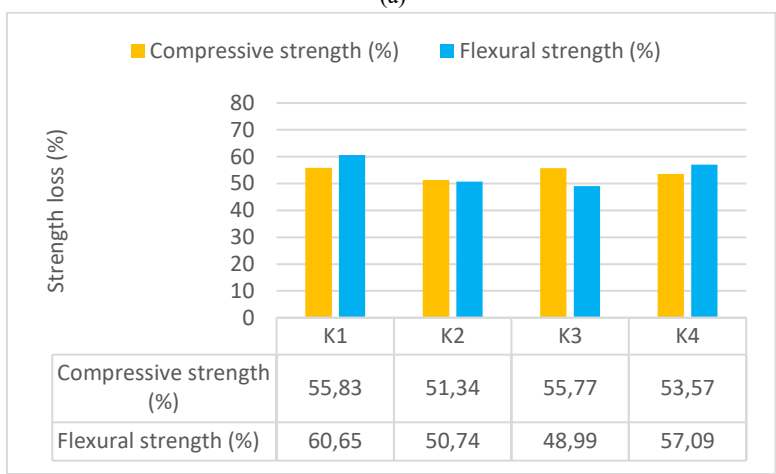


Fig. 7. Compressive and flexural strengths of SIFGEO (a) After 200 $^{\circ}$ C (b) After 400 $^{\circ}$ C (c) After 600 $^{\circ}$ C





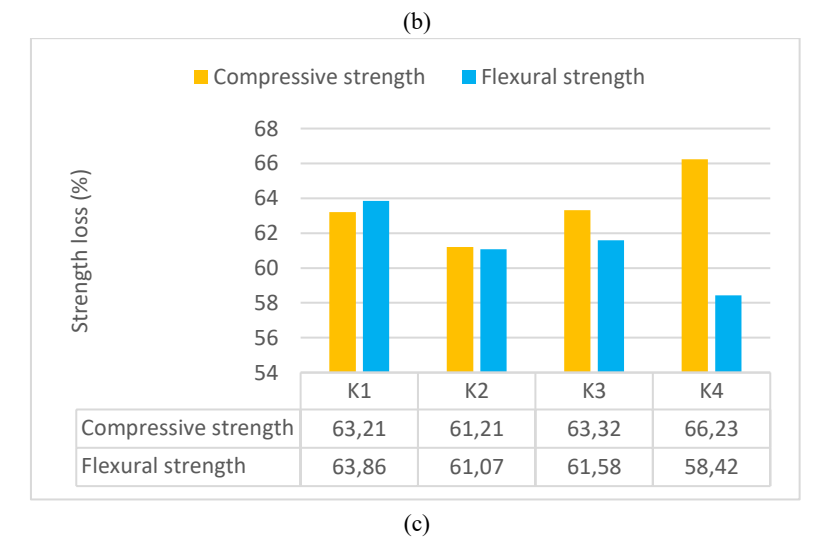


Fig. 8. Strength losses of SIFGEO (a) After 200 °C (b) After 400 °C (c) After 600 °C

Another remarkable result is that the losses in flexural strengths after 200 °C were higher than the compressive strengths. This result was attributed to the formation of microcracks in the mortar phase of the specimens. This is closely related to the fracture mechanics of ceramics because SIFGEO's geopolymer mortar is classified as ceramic. In the case of cracks in the internal structure of ceramic materials, stress concentrations occur when subjected to flexural loads [67]. These stress concentrations around the cracks cause the flexural strength to be more sensitive than the compressive strength. As the temperature applied to the specimens increased, the strength losses in both mechanical tests were close. It can be interpreted that these results were observed because the cracks in the SIFGEO mortar grew to macro size with increasing temperature. All groups lost a certain amount of strength after the 200 °C temperature application. This is due to the evaporation of water in the capillary gaps and microstructure to form cracks. When the temperature was increased to 400 °C, the crack formation accelerated, and the gel structures forming the skeleton of SIFGEO mortar disintegrated (dehydration). After a high temperature of 400 °C, the main reason for losing more than 50% of flexural and compressive strengths was the deformation of the bond structures. When the applied temperature was increased to 600 °C, the degradation increased further, with strength losses reaching 70%. Notably, the SIFGEO specimens produced offered satisfactory compressive and flexural strength even after exposure to temperatures as high as 600 °C. These results demonstrate the superiority of SIFGEO technology and its usability in applications.

Fig. 9 shows the fracture energies and flexural strengths of SIFGEO specimens after high temperatures were applied. When the results of the fracture energies are analyzed, the increase in temperature causes the fracture energies to decrease. The fracture energies of SIFGEO mixtures exposed to 600 °C decreased by more than 60% compared to those not exposed to temperature. These results are interpreted as a result of the physicochemical changes experienced by the mortar phase. After the 200 °C-exposed specimens were removed from the oven, map-shaped fine cracks were observed on the specimen surfaces, but there was no color change in the mortar phase. The reason for the formation of cracks is the evaporation of water in the pore structure, as explained above, causing parasitic stresses in the internal structure. After 200 °C temperature, the SIFGEO specimens were between 17% and 37%. After 400 °C high-temperature application, it was observed that the number and width of cracks in the samples increased. In addition, it was observed that the gray surfaces of the specimens turned brown in places. At this temperature value, it was thought that capillary water mostly evaporated, and dehydration started to occur in the gel structures. As a result of 400 °C treatment, a decrease of up to 55% in the fracture energy of SIFGEO samples was measured. When the temperature was increased to 600 °C, fracture energy losses reached their highest values. After this temperature, fracture energies decreased by more than 60%. At 600 °C, the first observation was that the color change was quite high. The mortar phases intensely turned brown after the SIFGEO mixtures were exposed to this temperature. In addition, the width of the cracks in the specimens increased significantly. The reason for the significant decrease in fracture energies and the physical change was interpreted as a serious deterioration of the gel structures. In addition, a color change was observed in some steel fibers after this temperature application. It is thought that oxidation of steel fibers at these temperatures also has a share in the measured losses. The variations in fracture energies with binder type were similar to the compressive and flexural strength losses. Fracture energies were generally higher for the BFS-based specimens, which aligns with the compressive and flexural strength results. With the use of BFS as a binder, the fracture energy increased, as did the other mechanical properties, as the number of bonds increased. As in the flexural and compressive strengths, the metakaolin-doped K3 mixture experienced less strength loss at temperatures of 400 °C and above. Therefore, the fracture energy of this group was measured to be higher than the others. From this point of view, it can be interpreted that the high-temperature resistance of MK-based polymeric bonds is slightly higher than the others.

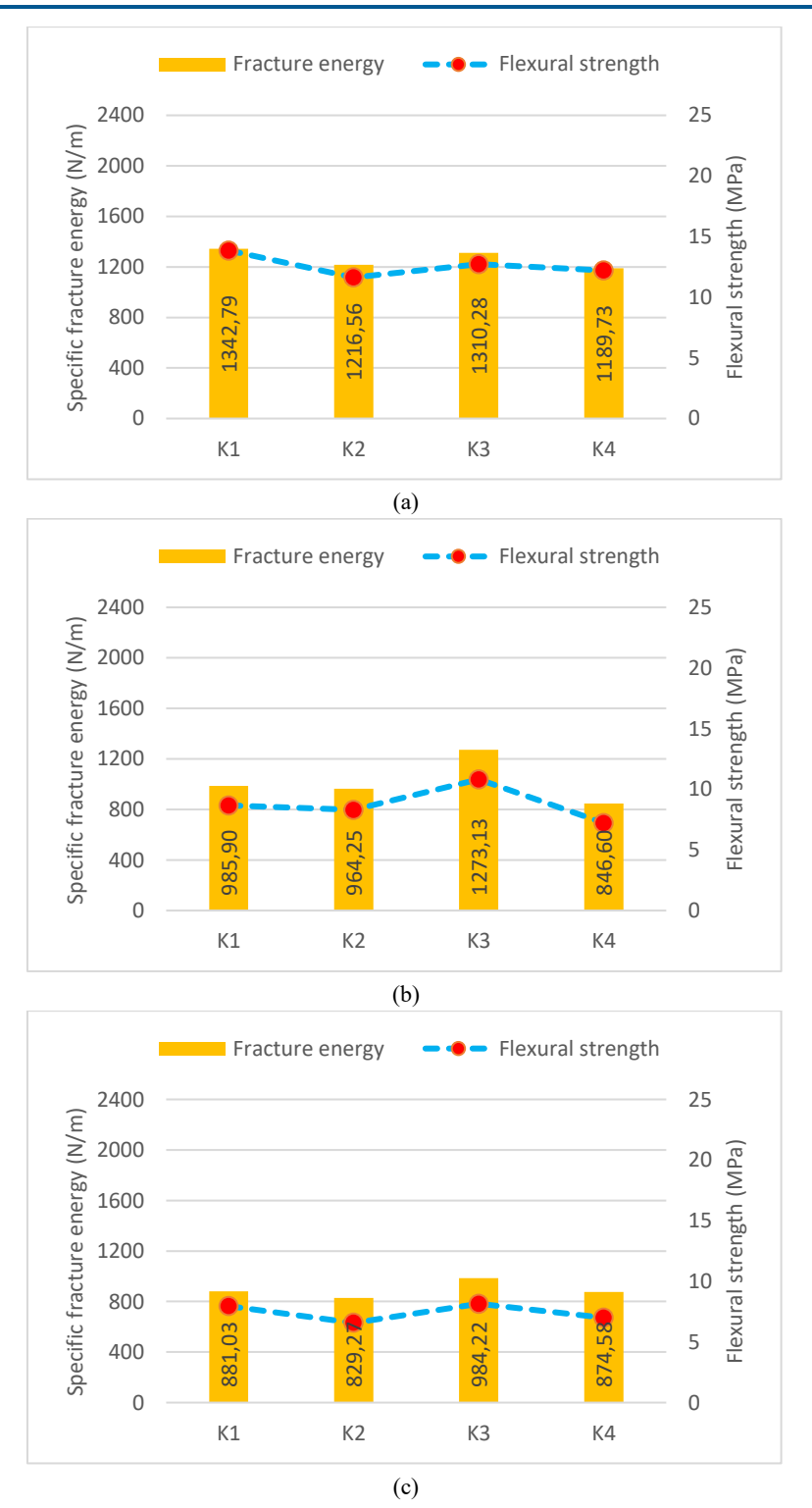


Fig. 9. Fracture energies of SIFGEO (a) After 200 °C (b) After 400 °C (c) After 600 °C

Fig. 10 presents the load-deflection graphs of all mixture samples that were subjected to high temperature. The main reason for the decrease in load values in the presented graphs has been explained in detail above, which is the deterioration of the internal structure of the mortar phase. The most important part of these graphs is each specimen's deflection after high-temperature application. If the load-deflection graph of each SIFGEO group is examined, although the deflection against the maximum load decreases with increasing temperature, the specimen continues to carry the load. In other words, although applying high temperature significantly reduces the strength properties, the deflection capacity of the specimens has not changed much. For example, while the maximum deflection value of the K1 specimen, which was not exposed to high temperature, was 33 mm, this value was measured as 31 mm in the specimen of the same group exposed to 600 °C. Similarly, in the K2 mixture, these values were approximately 33 and 30 mm, respectively. The fact that the deflection did not change much even after high temperature is a superior feature provided by dense fibers. Despite the physicochemical deterioration in the mortar phase, it was observed that the fibers still controlled the crack formation and propagation. In addition, the fact that the steel fibers did not degrade at the temperatures applied in the experiments also helped to stabilize the stresses.

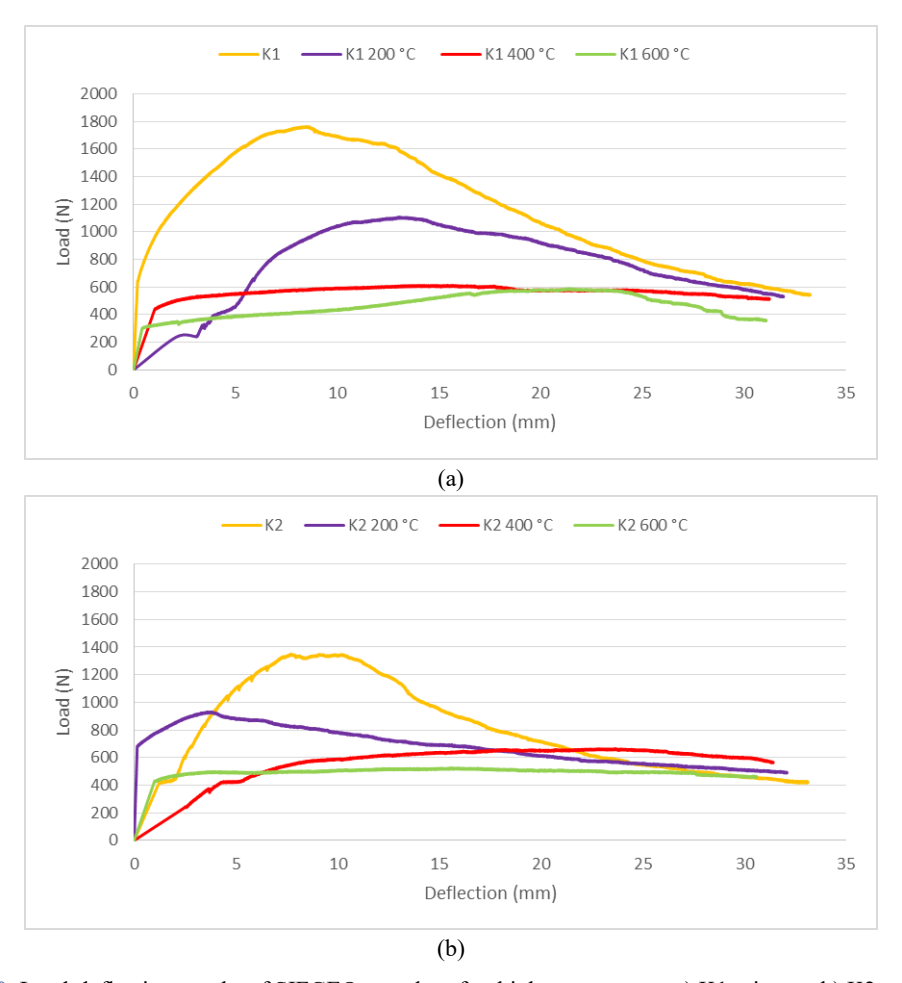


Fig. 10. Load-deflection graphs of SIFGEO samples after high temperature: a) K1 mixture, b) K2 mixture, c) K3 mixture, d) K4 mixture

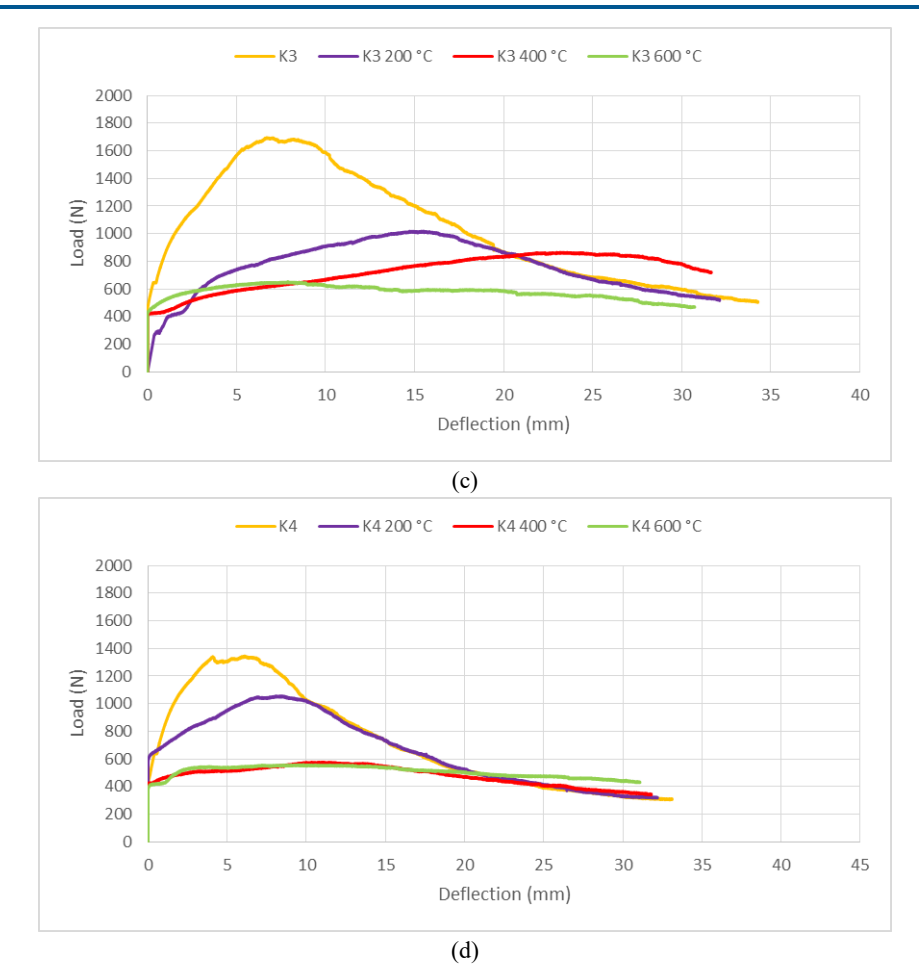


Fig. 10. Continued

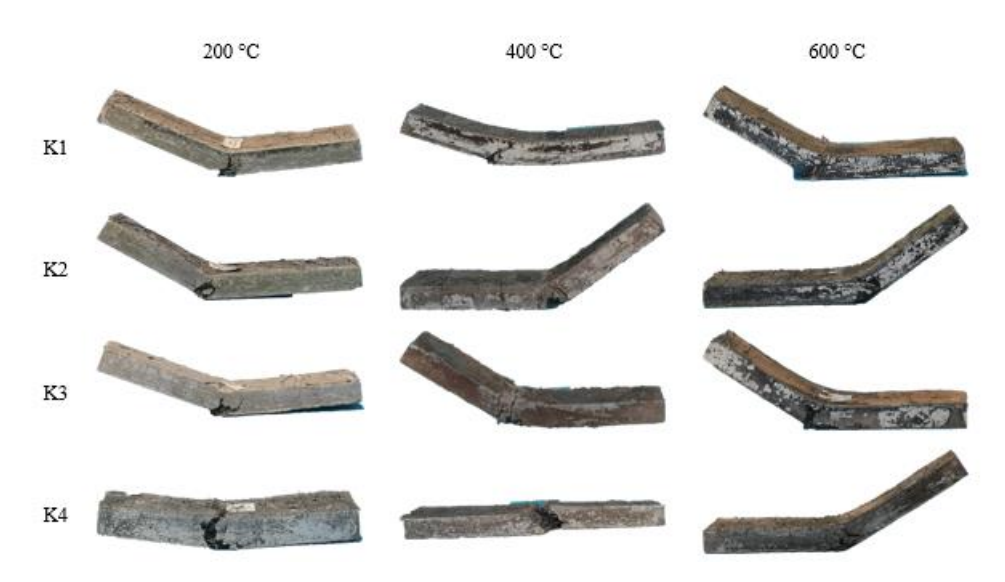


Fig. 11. Failure modes of SIFGEO specimens after high temperatures

Fig. 11 shows the fracture modes of the specimens subjected to high-temperature treatment at the end of the flexural test. Just as in Fig. 6 (b), the specimens did not fail in a brittle manner but could not carry the load after considerable deflection. The ductile fracture of the specimens, even after the high temperatures applied, can be considered another superior feature of SIFGEO. Bayraktar et al. [68] investigated the mechanical properties of furnace slag and silica fume-based alkali-activated SIFCOM specimens after 200, 400, 600, and 800 °C high-temperature treatment. Their research stated that the strength of the groups in which they used slag as a binder was better after high temperatures than those with silica fume. In addition, they measured that the toughness values of the specimens with BFS after high-temperature application were better than those with SF. Beglarigale et al. [69] investigated the flexural strength of cementitious SIFCON after high temperatures. After applying standard or steam curing to the test specimens, they applied 300, 600, 750, and 900 °C high temperatures. According to the test results, they did not observe any strength loss in the specimens applied at 300 °C, but they reported that the strength losses due to the increase in temperature reached significant dimensions. They also measured less strength loss in steam-cured specimens compared to standard-cured specimens. Ali et al. [70] investigated the mechanical and high-temperature properties of cement-based SIFCON specimens with 5%, 7.5%, and 10% steel fiber content. They applied for high temperatures at 200, 400, and 600 °C. They stated that the 7.5% fiber ratio specimens gave the best results in both mechanical tests and high-temperature resistance. Shaikh and Hosan [71] investigated the hightemperature strength of fly ash-based steel fiber geopolymer specimens. They used a sodium (Na) activator in one group and a potassium (K) activator in another to activate the inorganic component. The high temperatures in their studies were 200, 400, 600, and 800 °C. As a result of their experiments, they observed that the mechanical properties of the samples produced with the Na-sourced activator started to decrease after 200 °C. In comparison, this decrease started after 400 °C in the samples produced with the K-sourced activator.

3.3. Statistical analysis

Fig. 12(a) shows the results of R2 between flexural strength and fracture energy of all four mixtures, non-high temperature exposed and high temperature exposed specimens. For specimens K1, K2, K3, and K4, the R2 values were 0.96, 0.86, 0.98, and 0.92, respectively. These results show a high correlation between flexural strength and fracture energies, depending on the type of binder used in SIFGEO mixtures and the applied temperatures. The graphs presented in Fig. 6(a) and Fig. 7 are indicative of the strong relationship measured. If the graphs mentioned above are analyzed, it is seen that the changes in flexural strength affect the fracture energy to a great extent.

Fig. 12(b) presents the relationship between flexural strength and fracture energy of SIFGEO specimens, regardless of the type of binder. For the creation of this graph, the flexural strengths and fracture energies obtained at different temperatures in all groups were considered as a single data set (group). The graph equation created by the mentioned method is presented in the figure, and the R2 value was measured at 0.84. In light of the results obtained, it was determined that there is a high correlation between the flexural strength and fracture energy of the specimens produced with SIFGEO technology, regardless of the type of binder used in mortar production. Lee [72] investigated the mechanical properties of beams with different flexural strengths and fiber contents. As a result of his experimental study, he observed that the beams with the highest flexural strength and higher fiber content had higher energy absorption. Based on these results, the author stated that there is a good relationship between flexural strength and energy absorption. Zhao et al. [73] added four different types of fibers to fly ash and slag-based geopolymer concretes. As a result of their research, they reported a high correlation between the flexural strength and fracture energy of specimens with each type of fiber.

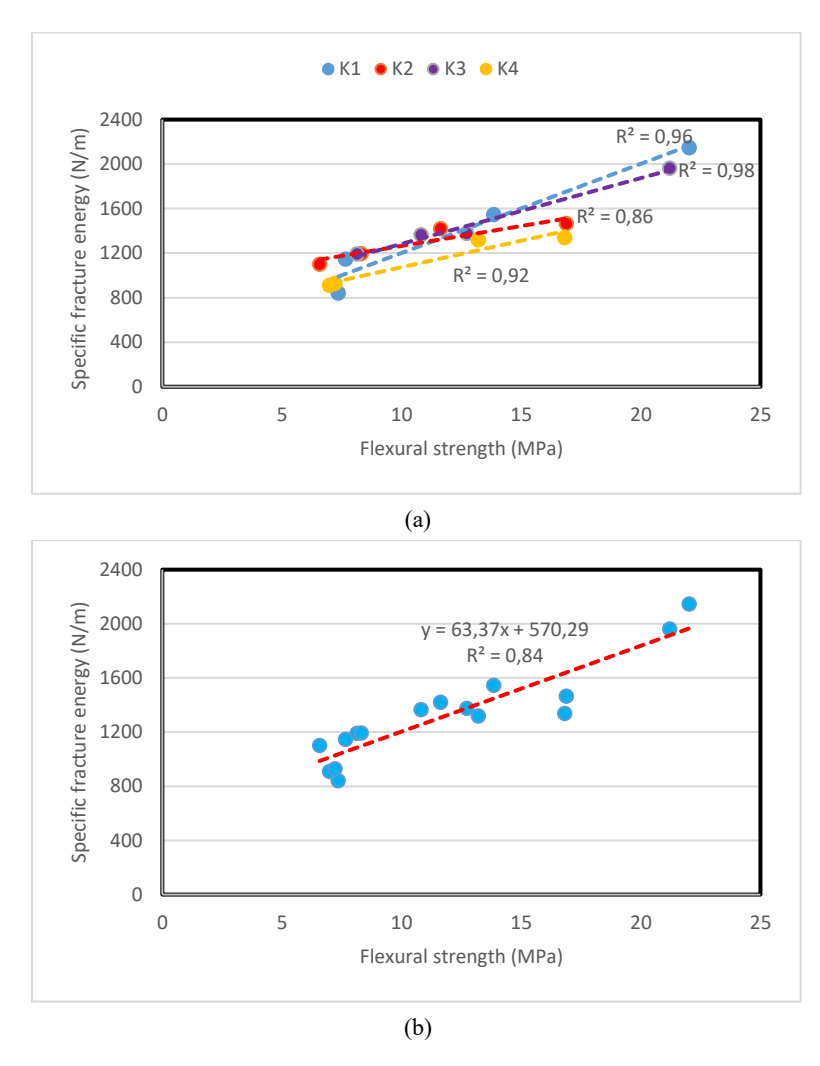


Fig. 12. Relationship with flexural strength and fracture energy of SIFGEO specimens

Fig. 13(a) shows the R2 values between flexural strength and compressive strength of specimens of four different mixtures with and without exposure to high temperature. For specimens K1, K2, K3, and K4, these values were 0.89, 0.96, 0.94, and 0.96, respectively. These data show a powerful relationship between flexural strength and compressive strength depending on the type of binder used in SIFGEO mixtures and the applied temperatures. The graphs presented in Fig. 4 and Fig. 7 also evidence this strong relationship. When these graphs are analyzed, it is seen that the changes in flexural strength significantly affect compressive strength.

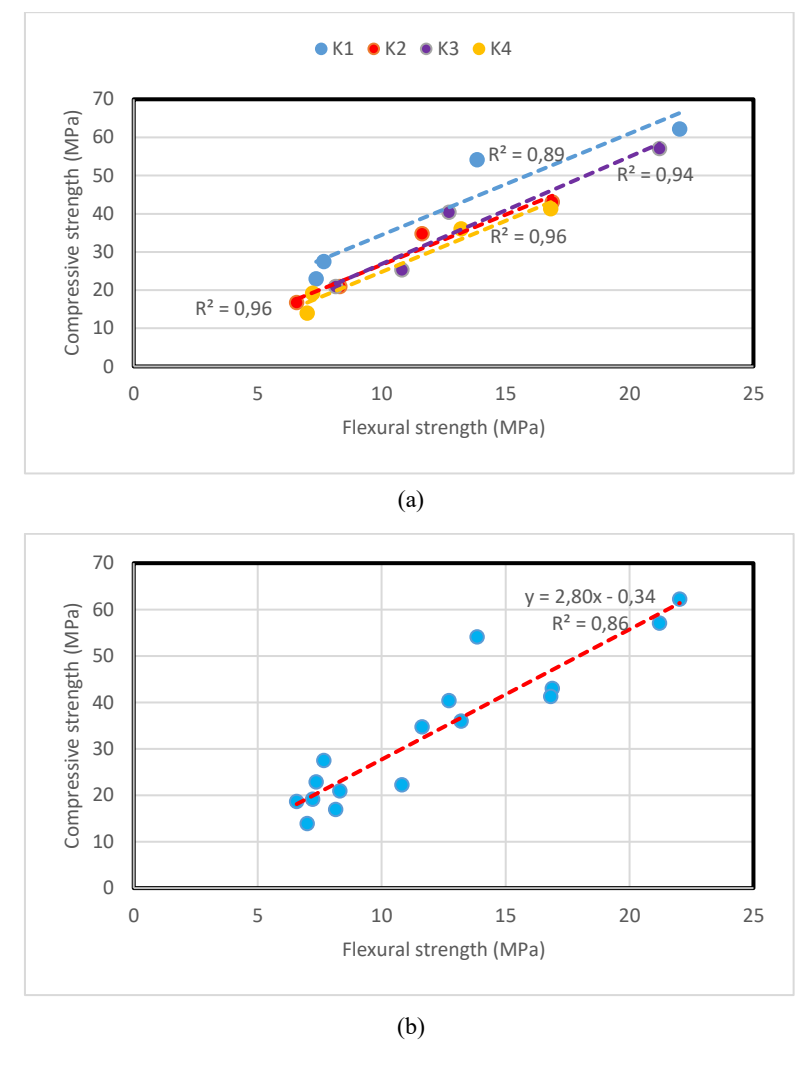


Fig. 13. Relationship with flexural strength and compressive strength of SIFGEO specimens

Fig. 13(b) shows the relationship between flexural strength and compressive strength of SIFGEO specimens, regardless of binder type. To generate this graph, the flexural and compressive strengths obtained at different temperatures were considered a single data set. The R2 value of the equation presented in the graph was measured as 0.86. As a result, it was found that there is a high correlation between flexural strength and compressive strength in specimens produced with SIFGEO technology, regardless of the type of binder used in mortar production. In their experimental study, Xu and Shi [74] investigated the relationship between compressive strength and flexural strength of polypropylene fiber and glass fiber-reinforced concrete. According to their experimental results, a relationship of 0.8 was obtained between compressive strength and flexural strength. Parashar et al. [75] investigated the mechanical properties of blast furnace slag-based geopolymer concretes with different proportions of steel fiber. The researchers reported a high correlation between the composite's flexural strength and compressive strength.

4. Conclusions

The main objective of this study is to investigate the mechanical and high-temperature behavior of SIFGEO specimens produced by combining geopolymer and SIFCON technology. Within the scope of the study, the effect of three different high temperatures (200, 400, and 600°C) on the specimens produced using geopolymer mortar phase with four different binder contents was experimentally measured. The following results were obtained in the study are as follows:

- Among the SIFGEO specimens not exposed to high temperature, the highest compressive and flexural strengths were measured in the mixture using only blast furnace slag as a binder. The compressive and flexural strength values in the K1 mix were 64.24 and 22 MPa, respectively.
- The highest fracture energy value among SIFGEO specimens not exposed to high temperature was measured in the K1 specimen with a value of 2146.62 N/m.
- In SIFGEO samples exposed to 200 °C, sample K1 measured the highest compressive and flexural strengths, with results of 54.15 and 13.85 MPa, respectively.
- When the temperature was increased to 400 °C and 600 °C, the compressive strengths of K1 and K3 specimens were very close, while these values were lower for K2 and K4 specimens. In addition, the flexural strength results of the K3 specimen are slightly higher than K1 at these temperature values.
- At 200 °C, the loss of flexural strength in SIFGEO specimens was higher than the loss of
 compressive strength. At 400 and 600 °C, the reduction rates in compressive and flexural strengths
 became similar, indicating that the degradation mechanisms at these higher temperatures affected
 both properties to a comparable extent.
- After a 200 °C temperature application, the highest fracture energy value was measured in the K1 specimen, 1342.79 N/m. When the temperature was increased to 400 °C and 600 °C, the highest fracture energy values belonged to the K3 specimen, 1273.13 and 984.22 N/m, respectively. In addition, despite being exposed to high temperatures, the dense fibers in the mixtures kept the deflection values high.
- Depending on the type of binder and the applied temperature, a high relationship was found between
 flexural strength and fracture energy, and between flexural strength and compressive strength. In
 addition, a high relationship was observed between flexural strength fracture energy and
 compressive strength, depending only on the applied temperature but not on the type of binder.

In conclusion, this study has demonstrated that SIFGEO can be considered a potential innovation in the construction industry and offers significant advantages regarding sustainability and performance. Future research should be directed towards expanding the applications of this material and optimizing its performance. It also shows that SIFGEO should be carefully evaluated in structural applications, especially those likely to be exposed to high temperatures.

CRediT authorship contribution statement

Haluk Görkem Alcan: Writing – original draft, Writing-review and editing, Barış Bayrak: Methodology, Investigation, Data curation, Gökhan Kaplan: Writing-review and editing, Conceptualization, Abdulkadir Cüneyt Aydın: Supervision, Project administration, Conceptualization

Declaration of conflicting interests

The author(s) declared no potential conflicts of interest with respect to the research, authorship, and/or publication of this article.

Funding

No funding was received for this study.

Data availability statement

The datasets generated and/or analyzed during the current study are available from the corresponding author on reasonable request.

References

- [1] Agustí-Juan I, Müller F, Hack N, Wangler T, Habert G (2017) Potential benefits of digital fabrication for complex structures: Environmental assessment of a robotically fabricated concrete wall. J Clean Prod 154:330–340.
- [2] Hasar U, Simsek O, Aydin A (2010) Application of varying-frequency amplitude-only technique for electrical characterization of hardened cement-based materials. Microw Opt Technol Lett 52(4):801–805.
- [3] Farnam Y, Moosavi M, Shekarchi M, Babanajad S, Bagherzadeh A (2010) Behaviour of slurry infiltrated fibre concrete (SIFCON) under triaxial compression. Cem Concr Res 40(11):1571–1581.
- [4] Naaman AE, Homrich JR (1989) Tensile stress-strain properties of SIFCON. ACI Mater J 86(3):244–251.
- [5] Bencardino F, Rizzuti L, Spadea G, Swamy R (2010) Experimental evaluation of fiber reinforced concrete fracture properties. Compos B Eng 41(1):17–24.
- [6] Li VC, Maalej M (1996) Toughening in cement-based composites. Part II: Fiber-reinforced cementitious composites. Cem Concr Compos 18(4):239–249.
- [7] Yan A, Wu K, Zhang X (2002) A quantitative study on the surface crack pattern of concrete with high content of steel fiber. Cem Concr Res 32(9):1371–1375.
- [8] Balaji S, Thirugnanam G (2018) Behaviour of reinforced concrete beams with SIFCON at various locations in the beam. KSCE J Civ Eng 22:161–166.
- [9] Chun P-j, Lee SH, Cho SH, Lim YM (2013) Experimental study on blast resistance of SIFCON. J Adv Concr Technol 11(4):144-150.
- [10] Hamza AM, Naaman AE (1996) Bond characteristics of deformed reinforcing steel bars embedded in SIFCON. ACI Mater J 93(6):578–588.
- [11] Morishima S, Yamaguchi M, Shibuya S, Kaneyasu S, Sueishi T (2020) Effects of fiber type on blast resistance of slurry-infiltrated fiber concrete under contact detonation. J Adv Concr Technol 18(4):157–167.
- [12] Rao HS, Ghorpade VG, Ramana N, Gnaneswar K (2010) Response of SIFCON two-way slabs under impact loading. Int J Impact Eng 37(4):452–458.
- [13] Aydın AC, Alcan HG, Bayrak B, Kılıç M, Maali M (2020) The mechanical behavior of thermally enhanced polypropylene concrete. Constr Build Mater 262:120578.
- [14] Canbaz M (2014) The effect of high temperature on reactive powder concrete. Constr Build Mater 70:508–513.
- [15] Chan SY, Peng G-f, Chan JK (1996) Comparison between high-strength concrete and normal-strength concrete subjected to high temperature. Mater Struct 29:616–619.
- [16] Guo Y, Luo L, Liu T, Hao L, Li Y, Liu P, Zhu T (2024) A review of low-carbon technologies and projects for the global cement industry. J Environ Sci 136:682–697.
- [17] Alcan HG, Bayrak B, Öz A, Kavaz E, Kaplan G, Çelebi O, Aydın AC (2023) A comprehensive characterization on geopolymer concretes with low content slag and quartz aggregates: the shielding features. Radiat Eff Defects Solids 178(7–8):769–798.
- [18] Almutairi AL, Tayeh BA, Adesina A, Isleem HF, Zeyad AM (2021) Potential applications of geopolymer concrete in construction: A review. Case Stud Constr Mater 15:e00733.
- [19] Parathi S, Nagarajan P, Pallikkara SA (2021) Eco-friendly geopolymer concrete: A comprehensive review. Clean Technol Environ Policy 23:1701–1713.
- [20] Bayrak B, Kaplan G, Öz A, Kavaz E, Çelebi O, Alcan HG, Mohabbi M, Aydın AC (2023) Metakaolin-based geopolymer concretes for nuclear protection: On the perspective of physicochemical, durability, and microstructure. Struct Concr 24(5):6644–6671.

[21] Ma C-K, Awang AZ, Omar W (2018) Structural and material performance of geopolymer concrete: A review. Constr Build Mater 186:90–102.

- [22] Mohajerani A, Suter D, Jeffrey-Bailey T, Song T, Arulrajah A, Horpibulsuk S, Law D (2019) Recycling waste materials in geopolymer concrete. Clean Technol Environ Policy 21:493–515.
- [23] Türkmen I, Öz A, Aydın AC (2010) Characteristics of workability, strength, and ultrasonic pulse velocity of SCC containing zeolite and slag. Sci Res Essays 5(15):2055–2064.
- [24] Salas DA, Ramirez AD, Ulloa N, Baykara H, Boero AJ (2018) Life cycle assessment of geopolymer concrete. Constr Build Mater 190:170–177.
- [25] Al Bakri AM, Kamarudin H, Bnhussain M, Nizar IK, Rafiza A, Zarina Y (2012) The processing, characterization, and properties of fly ash-based geopolymer concrete. Rev Adv Mater Sci 30(1):90–97.
- [26] Imtiaz L, Rehman SKU, Memon SA, Khan MK, Javed MF (2020) A review of recent developments and advances in eco-friendly geopolymer concrete. Appl Sci 10(21):7838.
- [27] Alcan HG, Bayrak B, Öz A, Çelebi O, Kaplan G, Aydın AC (2024) Synergetic effect of fibers on geopolymers: Cost-effective and sustainable perspective. Constr Build Mater 414:135059.
- [28] Duxson P, Provis JL, Lukey GC, Mallicoat SW, Kriven WM, Van Deventer JS (2005) Understanding the relationship between geopolymer composition, microstructure and mechanical properties. Colloids Surf A Physicochem Eng Asp 269(1–3):47–58.
- [29] Wong LS (2022) Durability performance of geopolymer concrete: A review. Polymers 14(5):868.
- [30] Amran M, Huang S-S, Debbarma S, Rashid RS (2022) Fire resistance of geopolymer concrete: A critical review. Constr Build Mater 324:126722.
- [31] Tennakoon C, Shayan A, Sanjayan JG, Xu A (2017) Chloride ingress and steel corrosion in geopolymer concrete based on long term tests. Mater Des 116:287–299.
- [32] Türkmen İ, Karakoç MB, Kantarcı F, Maraş MM, Demirboğa R (2016) Fire resistance of geopolymer concrete produced from Elazığ ferrochrome slag. Fire Mater 40(6):836–847.
- [33] ASTM C230 (2021) Standard Specification for Flow Table for Use in Tests of Hydraulic Cement. ASTM International, West Conshohocken.
- [34] Alvarado C, Martínez-Cerna D, Alvarado-Quintana H (2023) Geopolymer made from kaolin, diatomite, and rice husk ash for ceiling thermal insulation. Buildings 14(1):112.
- [35] Aredes F, Campos T, Machado J, Sakane K, Thim G, Brunelli D (2015) Effect of cure temperature on the formation of metakaolinite-based geopolymer. Ceram Int 41(6):7302–7311.
- [36] Ürünveren H, Beycioğlu A, Resuloğulları EÇ, Dişken NB (2024) A comparative investigation of eco-friendly fly ash-based geopolymer mortar produced by using electrical and heat curing: Mechanical properties, energy consumption, and cost. Constr Build Mater 439:137200.
- [37] Öz A, Bayrak B, Kaplan G, Aydın AC (2023) Effect of waste colemanite and PVA fibers on GBFS-metakaolin based high early strength geopolymer composites (HESGC): Mechanical, microstructure and carbon footprint characteristics. Constr Build Mater 377:131064.
- [38] Zhang P, Wang K, Li Q, Wang J, Ling Y (2020) Fabrication and engineering properties of concretes based on geopolymers/alkali-activated binders: A review. J Clean Prod 258:120896.
- [39] ASTM C349 (2018) Standard Test Method for Compressive Strength of Hydraulic-Cement Mortars (Using Portions of Prisms Broken in Flexure). ASTM International, West Conshohocken.
- [40] ASTM C348 (2021) Standard Test Method for Flexural Strength of Hydraulic-Cement Mortars. ASTM International, West Conshohocken.
- [41] ASTM C1018 (2017) Standard Test Method for Flexural Toughness and First-Crack Strength of Fiber-Reinforced Concrete (Using Beam With Third-Point Loading). ASTM International, West Conshohocken.
- [42] ASTM E119 (2022) Standard Test Methods for Fire Tests of Building Construction and Materials. ASTM International, West Conshohocken.
- [43] Luo Z, Li W, Gan Y, Mendu K, Shah SP (2020) Applying grid nanoindentation and maximum likelihood estimation for NASH gel in geopolymer paste: Investigation and discussion. Cem Concr Res 135:106112.
- [44] Xu L-Y, Alrefaei Y, Wang Y-S, Dai J-G (2021) Recent advances in molecular dynamics simulation of the NASH geopolymer system: Modeling, structural analysis, and dynamics. Constr Build Mater 276:122196.

- [45] Matsimbe J, Dinka M, Olukanni D, Musonda I (2022) Geopolymer: A systematic review of methodologies. Materials 15(19):6852.
- [46] Puligilla S, Mondal P (2013) Role of slag in microstructural development and hardening of fly ash-slag geopolymer. Cem Concr Res 43:70–80.
- [47] Nath P, Sarker PK (2014) Effect of GGBFS on setting, workability, and early strength properties of fly ash geopolymer concrete cured in ambient condition. Constr Build Mater 66:163–171.
- [48] Bhavsar J, Panchal VR (2023) Strength and durability evaluation of multi-binder geopolymer concrete in ambient condition. KSCE J Civ Eng 27(4):1708–1719.
- [49] Wang Y, Liu X, Zhang W, Li Z, Zhang Y, Li Y, Ren Y (2020) Effects of Si/Al ratio on the efflorescence and properties of fly ash-based geopolymer. J Clean Prod 244:118852.
- [50] He P, Wang M, Fu S, Jia D, Yan S, Yuan J, Xu J, Wang P, Zhou Y (2016) Effects of Si/Al ratio on the structure and properties of metakaolin-based geopolymer. Ceram Int 42(13):14416–14422.
- [51] ACI Committee (2008) Building code requirements for structural concrete (ACI 318-08) and commentary. American Concrete Institute, Farmington Hills.
- [52] Meisuh BK, Kankam CK, Buabin TK (2018) Effect of quarry rock dust on the flexural strength of concrete. Case Stud Constr Mater 8:16–22.
- [53] Nguyen KT, Ahn N, Le TA, Lee K (2016) Theoretical and experimental study on mechanical properties and flexural strength of fly ash-geopolymer concrete. Constr Build Mater 106:65–77.
- [54] Ashour SA, Wafa FF, Kamal MI (2000) Effect of the concrete compressive strength and tensile reinforcement ratio on the flexural behavior of fibrous concrete beams. Eng Struct 22(9):1145–1158.
- [55] Kurt M, Aydin AC, Gül MS, Gül R, Kotan T (2015) The effect of fly ash to self-compactability of pumice aggregate lightweight concrete. Sadhana 40:1343–1359.
- [56] Lee J-H, Cho B, Choi E (2017) Flexural capacity of fiber reinforced concrete with a consideration of concrete strength and fiber content. Constr Build Mater 138:222–231.
- [57] Noushini A, Hastings M, Castel A, Aslani F (2018) Mechanical and flexural performance of synthetic fibre reinforced geopolymer concrete. Constr Build Mater 186:454–475.
- [58] Gok SG, Sengul O (2023) Mechanical properties of alkali-activated slag-based SIFCON incorporating waste steel fibers and waste glass. Constr Build Mater 408:133697.
- [59] Ipek M, Aksu M, Yilmaz K, Uysal M (2014) The effect of pre-setting pressure on the flexural strength and fracture toughness of SIFCON during the setting phase. Constr Build Mater 66:515–521.
- [60] Alcan HG, Bingöl AF (2019) Examining SIFCON's mechanical behaviors according to different fiber and matrix phase. Iran J Sci Technol Trans Civ Eng 43:501–507.
- [61] Bayraktar OY, Kaplan G, Shi J, Benli A, Bodur B, Turkoglu M (2023) The effect of steel fiber aspect-ratio and content on the fresh, flexural, and mechanical performance of concrete made with recycled fine aggregate. Constr Build Mater 368:130497.
- [62] Ding Y, Shi C-J, Li N (2018) Fracture properties of slag/fly ash-based geopolymer concrete cured in ambient temperature. Constr Build Mater 190:787–795.
- [63] Gomes RF, Dias DP, de Andrade Silva F (2020) Determination of the fracture parameters of steel fiber-reinforced geopolymer concrete. Theor Appl Fract Mech 107:102568.
- [64] Gümüş M, Bayrak B, Çelebi O, Alcan HG, Kaplan G, Öz A, Aydın AC (2023) The mechanical and fracture characteristics of low fiber content slurry-infiltrated fiber concrete. Iran J Sci Technol Trans Civ Eng 47(6):3345– 3356.
- [65] Güneyisi E, Gesoglu M, Özturan T, İpek S (2015) Fracture behavior and mechanical properties of concrete with artificial lightweight aggregate and steel fiber. Constr Build Mater 84:156–168.
- [66] Jung H, Park S, Kim S, Park C (2017) Performance of SIFCON-based HPFRCC under field blast load. Procedia Eng 210:401–408.
- [67] Königsberger M, Pichler B, Hellmich C (2014) Micromechanics of ITZ-aggregate interaction in concrete part I: stress concentration. J Am Ceram Soc 97(2):535–542.
- [68] Bayraktar OY, Bozkurt TH, Benli A, Koksal F, Türkoğlu M, Kaplan G (2023) Sustainable one-part alkali activated slag/fly ash Geo-SIFCOM containing recycled sands: Mechanical, flexural, durability and microstructural properties. Sustain Chem Pharm 36:101319.

[69] Beglarigale A, Yalçınkaya Ç, Yiğiter H, Yazıcı H (2016) Flexural performance of SIFCON composites subjected to high temperature. Constr Build Mater 104:99–108.

- [70] Ali MH, Atiş CD, Al-Kamaki YSS (2022) Mechanical properties and efficiency of SIFCON samples at elevated temperature cured with standard and accelerated method. Case Stud Constr Mater 17:e01281.
- [71] Shaikh FUA, Hosan A (2016) Mechanical properties of steel fibre reinforced geopolymer concretes at elevated temperatures. Constr Build Mater 114:15–28.
- [72] Lee J-H (2017) Influence of concrete strength combined with fiber content in the residual flexural strengths of fiber-reinforced concrete. Compos Struct 168:216–225.
- [73] Zhao C, Wang Z, Wu X, Zeng X, Zhu Z, Guo Q, Zhao R (2023) Study on the flexural properties and fiber-selection method of fiber-reinforced geopolymer concrete. Struct Concr 24(1):1364–1385.
- [74] Xu B, Shi H (2009) Correlations among mechanical properties of steel fiber reinforced concrete. Constr Build Mater 23(12):3468–3474.
- [75] Parashar AK, Kumar A, Singh P, Gupta N (2024) Study on the mechanical properties of GGBS-based geopolymer concrete with steel fiber by cluster and regression analysis. Asian J Civ Eng 25(3):2679–2686.